Journal of Nuclear Materials 392 (2009) 531–544

Contents lists available at ScienceDirect

Journal of Nuclear Materials

journal homepage: www.elsevier.com/locate/jnucmat

Prototypical experiments relating to air oxidation of Zircaloy-4 at high temperatures

Martin Steinbrück *

Forschungszentrum Karlsruhe GmbH, Institute for Materials Research I, Postfach 3640, D-76021 Karlsruhe, Germany

ARTICLE INFO

Article history:
Received 4 March 2009
Accepted 22 April 2009

ABSTRACT

The mechanism of the reaction between Zircaloy-4 and air at temperatures from 800 to 1500 °C was studied. Air attack under prototypical conditions with air ingress during a hypothetic severe nuclear reactor accident was investigated. Oxidation in air and in air and nitrogen-containing atmospheres leads to a major degradation of the cladding material. The main mechanism is the formation of zirconium nitride and its re-oxidation. Pre-oxidation in steam prevents air attack as long as the oxide scale is intact. Under steam/oxygen starvation conditions, the oxide scale is reduced and significant external nitride formation takes place. When modeling air ingress in severe accident computer codes, parabolic correlations for oxidation in air may be applied only for high temperatures (>1400 °C) and for pre-oxidized cladding (⩾1100 °C). Under all other conditions, faster, rather linear reaction kinetics should be applied.

1. Introduction

Most investigations of core degradation during severe nuclear reactor accidents consider oxidation of metal core components by steam only. However, there are various scenarios of air having access to the core. Air ingress is possible under shutdown conditions when the reactor coolant system is open to the containment atmosphere. Air oxidation of the remaining outer core regions after reactor pressure vessel failure in the late phase of core degradation during severe accidents is another possible scenario [1]. Furthermore, the failure of a storage or transportation cask may result in air intrusion and subsequent interaction with the spent fuel rods.

The special impact of air ingress on reactor safety is due to:

- The vigorous oxidation and degradation of the remaining cladding. Zirconium oxidation by air releases about 85% more heat than oxidation by steam. The oxidation kinetics in air is much faster due to the formation of non-protective oxide (nitride) scales.
- The oxidation of the UO_2 fuel to U_3O_8, which results in a lower melting temperature and impairment of the mechanical stability of the fuel.
- The influence of air on the volatility of the fission products. In a highly oxidizing atmosphere, for instance, the formation of volatile ruthenium oxides is favored.

Experimental and analytical studies of air ingress were performed within the EC's 4th Framework Program projects OPSA [2] and COBE [3]. In the recent past, this topic was again examined in the USA, with emphasis on storage and transportation cask accidents [4]. Studies in Europe focused on shutdown scenarios and the late phase of severe accidents [5]. IRSN launched the MOZART program to investigate various zirconium alloys in air atmospheres at moderate temperatures (600–1200 °C) in connection with spent fuel storage pool accidents [6].

The available experimental data on air oxidation at higher temperatures are limited to the reaction in pure air. The more prototypical scenarios of air oxidation of zirconium alloys pre-oxidized in steam were investigated only very recently [6], whereas the reaction of zirconium alloys in mixed air–steam atmospheres has not yet been investigated at all. This report presents the results of investigations of air oxidation obtained from parametric small-scale separate-effects tests in the temperature range of 800–1500 °C. More general information on air ingress, including bundle test results, was published recently in [7,8]. The air ingress results of the QUENCH-10 large-scale bundle test performed at the Forschungszentrum Karlsruhe were reported in 2004 [9].

This paper summarizes the results presented in the report FZKA 7257 [10].

2. Experimental

2.1. Equipment

Two experimental setups were used: The BOX rig and a commercial thermal balance (TG) which are described in detail in [10].

All tests with steam-containing atmosphere were performed in the so-called BOX rig. This facility consists of a Bronkhorst gas supply system for Ar, air, and steam (0–4 mol/h each), a tube furnace

* Tel.: +49 7247 822517; fax: +49 7247 824567.
E-mail address: steinbrueck@imf.fzk.de

0022-3115/$ - see front matter © 2009 Elsevier B.V. All rights reserved.
doi:10.1016/j.jnucmat.2009.04.018

with maximum temperatures of 1700 °C, a quadrupole mass spectrometer (MS) Balzers GAM 300, and an air lock allowing for the exchange of specimens at reaction temperature and under a defined atmosphere. The offgas tube from the furnace to the MS was heated to about 150 °C in order to prevent steam condensation. The mass spectrometer allowed for the quantitative analysis of all gaseous reaction products, including steam. If applicable, the hydrogen release rate was used as a measure of the reaction kinetics.

Kinetic experiments were performed in a commercial thermal balance (NETZSCH STA-409) coupled to a quadrupole mass spectrometer (NETZSCH Aeolos) via a capillary. The gases (Ar, O_2, N_2, air) were fed into the lower part of the vertical tube furnace via Bronkhorst flow controllers. Argon entered the furnace via the balance containment. The reaction gases were directly injected into the reaction tube to prevent contamination of the balance and to ensure a well-defined gas mixture in the furnace. Only highly pure gases with <1 or 10 ppm impurities were used. Since the thermal balance was not designed to operate under steam-containing atmospheres, oxygen had to be used to simulate (pre-)oxidation in steam. Oxide scales resulting from the oxidation of Zircaloy in oxygen are known to be very similar to those formed in steam. A limited test series in the BOX rig with pre-oxidation in steam confirmed that the behavior of specimens pre-oxidized in oxygen and steam is comparable (see Section 3.5).

2.2. Specimens

Zircaloy-4 tube segments (10.75 mm outer diameter, 0.725 mm wall thickness) were investigated in all tests. Segments of 1 cm length were used in the TG tests. They were positioned vertically. In the BOX rig, 2-cm tube segments were suspended horizontally on a zirconia rod.

Both types of specimens were open at the ends. Consequently, oxidation of internal surfaces could not be avoided. Some tests, however, needed to be performed without internal oxidation. For this purpose, ten closed specimens were produced with electron beam-welded end cups. A thin (thin enough to exclude internal oxidation) hole in the center of the bottom cup prevented the pressure from building up in the specimens.

2.3. Test procedure

Argon was used as a carrier gas and reference gas for mass spectroscopy in all tests. Consequently, 'tests in pure air and steam atmosphere' were conducted in air–argon and steam–argon mixtures, respectively. The use of argon may have some influence on gas diffusion, especially in pores and cracks. This effect was not investigated in this work.

At the beginning of the BOX test series, the furnace was heated up to the temperature desired and all auxiliary heaters for the tubing, valves, and flanges were switched on. The mass spectrometer was calibrated in parallel. After inserting the specimen, the air lock was connected to the furnace and flushed with argon. When the mass spectrometer indicated the absence of residual air in the furnace, the specimen was slowly pushed into the hot center of the furnace and thermally equilibrated before the desired gas mixture was switched on. To avoid strong temperature overshooting at high temperatures (⩾1200 °C), the specimens were shifted into the furnace in an (oxidizing) atmosphere, kept at their position at 1100 °C for one minute (resulting in a pre-oxidation of ~15 μm), and only then pushed into the hot zone. At the end of the isothermal oxidation period the gas flow was changed from the oxidizing gas or gas mixture to pure argon. The specimen was pulled back into the air lock, where it quickly cooled down and was exchanged by a new one. Fig. 1 illustrates the course of the test series at 1000 °C under various air–steam mixtures.

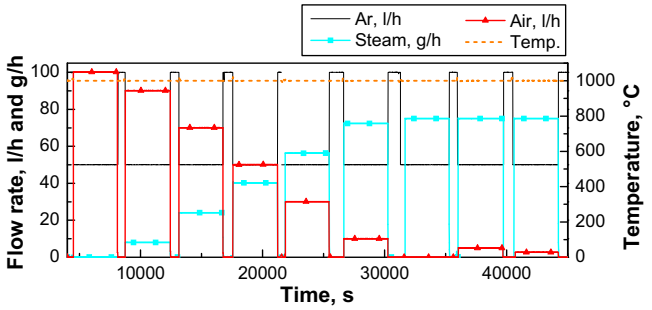

Fig. 1. Course of a series of tests at 1000 °C under different air–steam mixtures in the BOX rig, as reflected by the temperatures and gas flow rates.

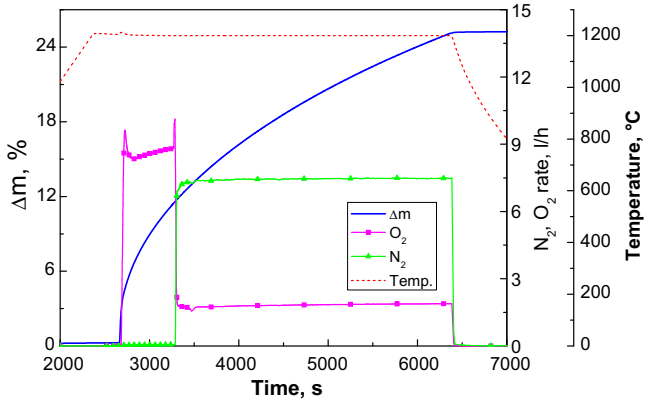

Fig. 2. Example of a test conducted in the thermal balance with pre-oxidation in oxygen followed by oxidation in air at 1200 °C.

The flow rate of the argon reference gas was usually 50 l/h. The air and nitrogen flow rates varied between 0 and 100 l/h, and steam was injected at 0–75 g/h. The masses of the specimens were measured before and after all tests.

In the thermal balance the specimens were heated to the desired temperature at a rate of 30 K/min under argon. Then, they were thermally equilibrated for 5 min. Subsequently, the oxidizing gas (mixture) was injected until a mass gain of ~25 wt% was reached or for a pre-defined time. The tests were completed by switching off the oxidizing gases and cooling the furnace as fast as possible with an argon atmosphere.

Complete oxidation of Zircaloy leads to a mass gain of 35 wt%. The mass gain of 25 wt% desired resulted in an adequate test duration and left a sufficient amount of the metal phase for metallographic examinations.

The argon flow rate was 10 l/h in all tests. Typical flow rates of oxygen, nitrogen, and air were also 10 l/h. At 1400 °C, some tests were conducted with 30 l/h air or oxygen to prevent oxygen starvation conditions from developing. Pre-oxidation was partly done with 3 l/h oxygen. Fig. 2 shows a typical test with pre-oxidation in oxygen and subsequent reaction in air.

The main parameters of all tests conducted are compiled in [10].

2.4. Post-test examinations

Photo macrographs of all specimens were produced after the tests. Then the specimens were embedded in epoxy resin, cut, ground, and polished for metallographic examination by optical

microscopy. Some specimens were investigated by SEM/EDX to detect nitride phases.

As was already mentioned above, most of the specimens were open, leading to inner and outer oxidation. As the experimental conditions, e.g., in terms of gas flow, are better defined for the external surface of the tube segments and as external oxidation is what occurs in reactors, the focus is on the external oxide scale.

3. Results

3.1. Tests in oxygen, nitrogen, and air

Reference tests were conducted in oxygen, nitrogen, and air at 800, 1000, 1200, and 1400 °C using the thermal balance. Fig. 3 shows the reaction rates obtained by means of TG tests. Generally, the reaction rate in a nitrogen atmosphere is much smaller (by about two orders of magnitude) than in oxygen or air. At 800 °C, the oxidation kinetics in air and oxygen is parabolic and identical for about one hour. Then, the reaction in air accelerates significantly and switches to a linear behavior. After about 3.5 h, the linear reaction coefficient again increases by a factor of two. The oxidation kinetics in oxygen remains parabolic for about 4.5 h, before a transition to rather linear behavior is observed. This transition is caused by breakaway oxidation [11], i.e., the transition from dense, protective oxide scales to cracked and less protective oxide scales. This effect is strongly accelerated in air due to the influence of nitrogen (see Section 4). The behavior at 1000 °C is quite similar. The transition from parabolic to faster kinetics takes place earlier (after about 200 and 2000 s in air and oxygen, respectively), but the kinetics in air is still remarkably faster, although less oxygen is available.

At 1200 °C, the reaction in oxygen follows parabolic kinetics during the whole test (no breakaway at temperatures above 1050 °C). An initially enhanced reaction rate is caused by a small temperature increase due to the strongly exothermic reaction. The reaction kinetics in air is intermediate between linear and parabolic. At the beginning of the reaction, it is slower than in pure oxygen due to the limited oxygen supply. At 1400 °C, the reaction kinetics is determined even more by different oxygen concentrations of the two gases supplied, and the reaction in pure oxygen is first faster than and finally equal to the reaction in air.

According to the post-test examination, degradation was greatest for the specimens oxidized in air, whereas the specimens exposed to nitrogen were almost unchanged; metallic in appearance with a more or less golden color. Micrographs (Fig. 4) clearly show typical breakaway effects such as undulating interface between metal and oxide and circumferential cracks in the oxide scale of the specimens oxidized in air and oxygen at 800 and 1000 °C. Gold-colored nitride phases are observed after oxidation in air at all temperatures. The specimen oxidized in air at 1400 °C only showed a local formation of nitride at locations of defective oxide scale. In general, however, the specimen was very similar to the specimen oxidized in oxygen at that temperature.

As already evident from the TG curves, the reaction of Zircaloy-4 with pure nitrogen is only marginal in comparison to that with air. No nitride was detected in such specimens, although macroscopically they were of golden color. In accordance with the Zr–N phase diagram [13], a superficial α-Zr(N) layer formed on all specimens in pure nitrogen. Note that the reaction times at 1200 and 1400 °C were much longer for the nitrogen specimens than for those in oxygen and air. At present, it is not clear whether the α-Zr(N) phase also contains oxygen which, e.g., may slowly diffuse through the alumina reaction tube at higher test temperatures.

The local initiation of nitrogen attack and the transition of the specimens to a layer-like structure with increasing temperature (and time) are illustrated in Fig. 5. Here, specimens are shown after 10 min oxidation in pure air at 1200–1500 °C in the BOX rig. Additionally, this series of images shows a coarsening of the oxide

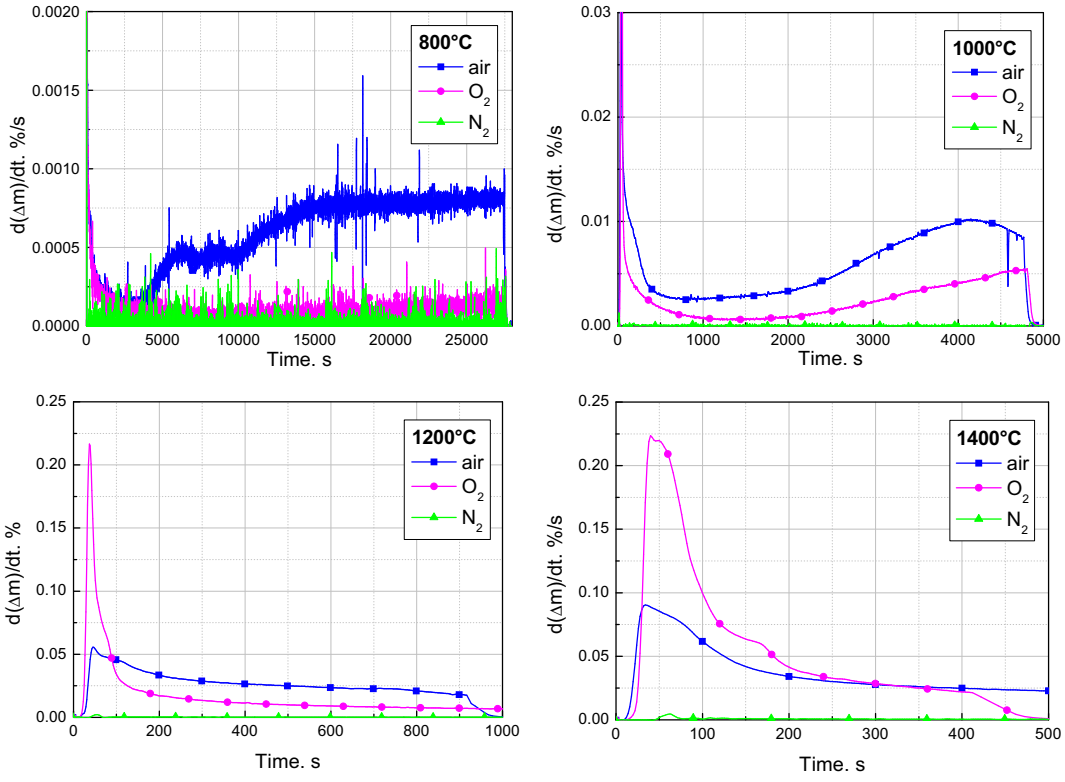

Fig. 3. Reaction rates of Zircaloy-4 in air, oxygen, and nitrogen at various temperatures.

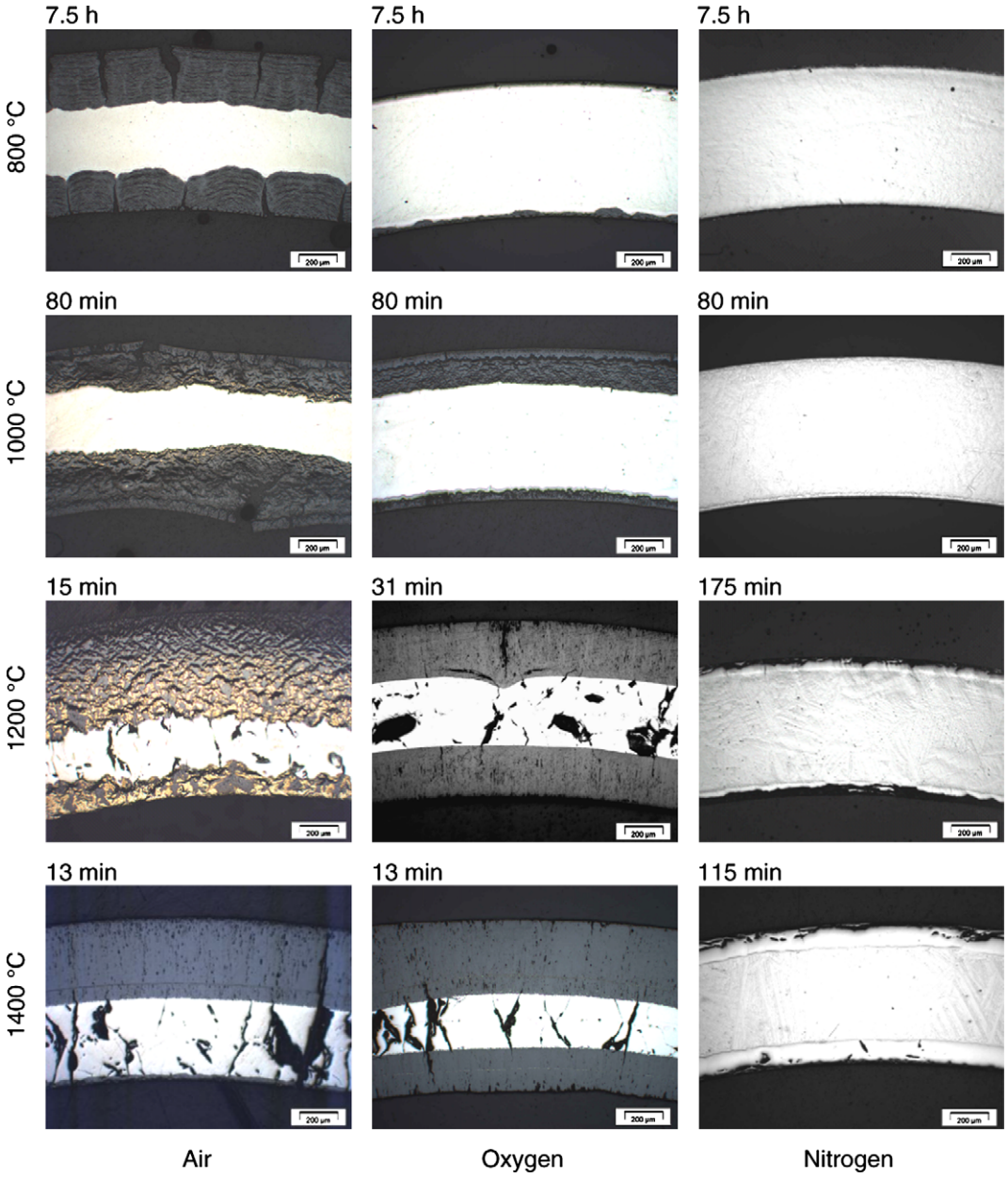

Fig. 4. Micrographs of the Zircaloy-4 specimens after reaction in different atmospheres. The approximate reaction times are indicated above the pictures.

morphology with temperature and finally a reversal of the trend of increasing degradation with rising temperatures at 1500 °C. At the latter temperature, the oxide scale is dense and looks very similar to that obtained in pure steam.

3.2. Tests in mixed air–steam atmospheres

An extensive study of the oxidation of Zircaloy-4 in mixed air–steam atmospheres was performed in the BOX rig. Between 800 and 1200 °C, 1-h isothermal tests and between 1200 and 1500 °C (with 100 K steps), 10-min isothermal tests were carried out using nine different atmospheres of pure air and pure steam and mixtures of both, yielding a total of 81 tests.

During all tests, the reaction gases in the offgas system were analyzed by MS. Fig. 6 illustrates some examples at various temperatures in steam and air–steam atmospheres. At 1000 °C, hydrogen was produced during the test in pure steam only. At 1500 °C, hydrogen was released in all tests with less than 50 vol.% air in the mixture. Under these conditions, the oxygen is consumed completely, initially at least, and steam oxidation can take place. The lower right diagram in Fig. 6 presents the transition from oxygen starvation conditions with hydrogen release to conditions with an excess of oxygen and suppression of hydrogen production. This figure also shows the discontinuities in the gas release curves at 1000 °C, which are caused by the breakaway effect.

In all tests the masses of the specimens were measured before and after oxidation. For the reasons described above, hydrogen release could not be used as measure of the degree of oxidation as it had been done in experiments under pure steam. Hence, the mass gain is the only integral figure of oxidation. At 800 °C, no influence of air in the mixture was observed although pure air caused an increase in the mass gain by about a factor of two after 1 h isothermal oxidation. At 900 °C, the influence of air was first detected at 90% air. Fig. 7 shows a more continuous transition between pure steam and pure air at higher temperatures. This means that even low amounts of steam in the mixture influence the oxidation

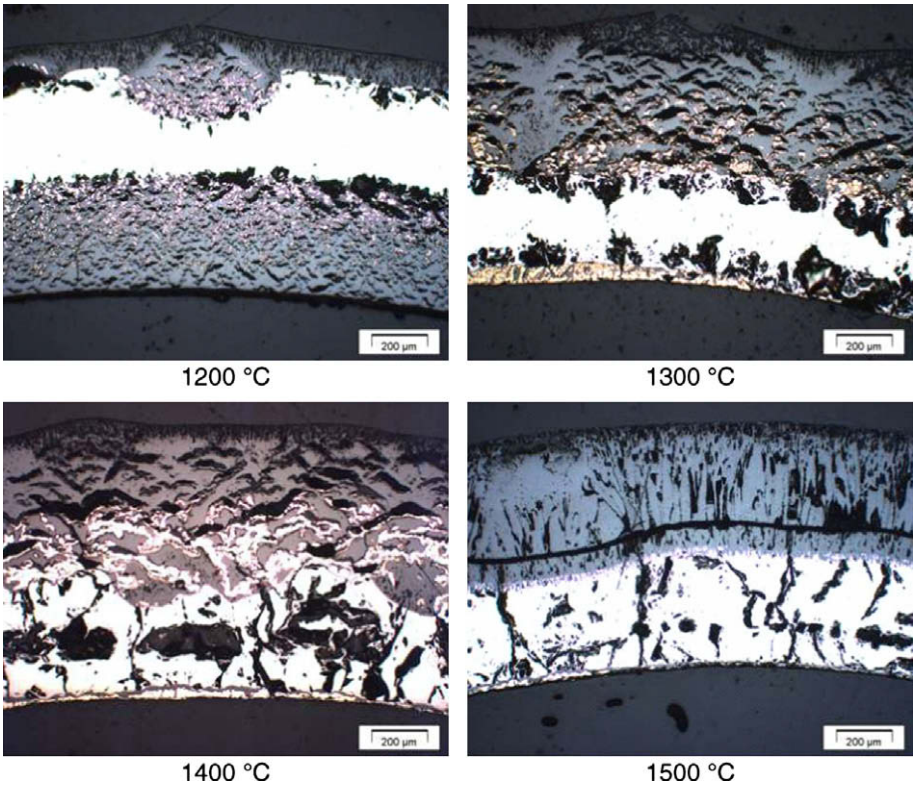

Fig. 5. Comparison of specimens oxidized in pure air for 10 min at various temperatures.

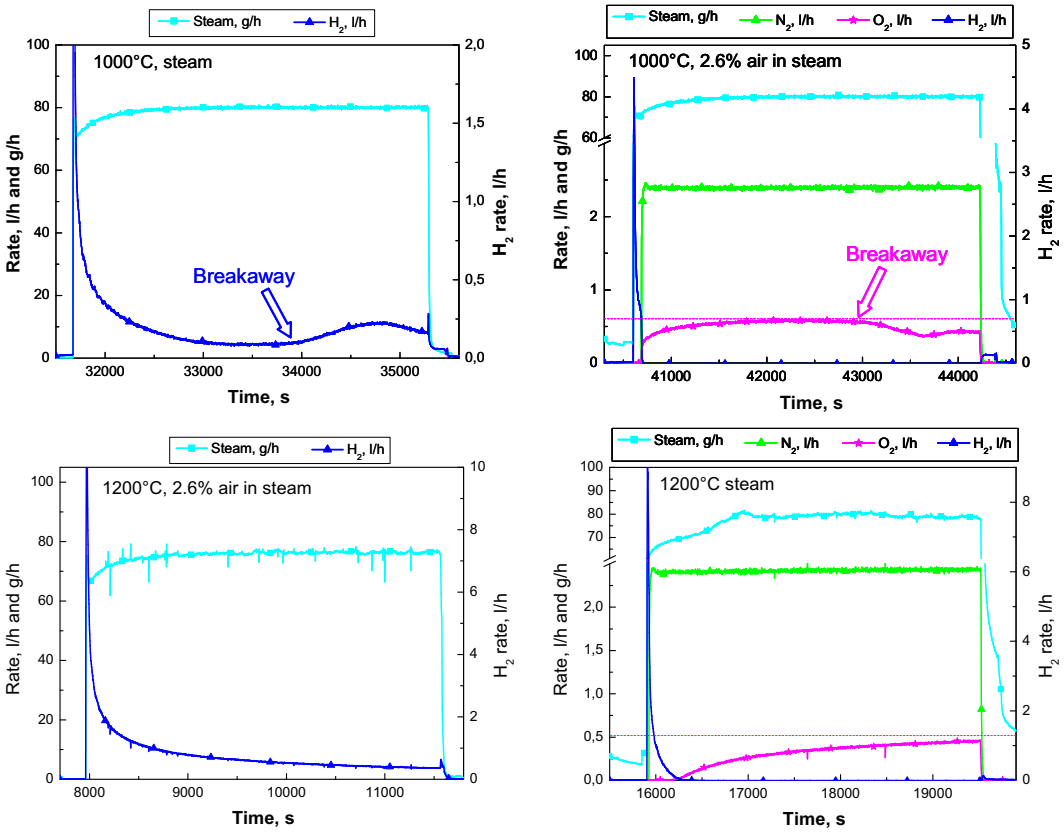

Fig. 6. MS results of tests in pure steam and in an air–steam mixture with a low air content at 1000 and 1200 °C.

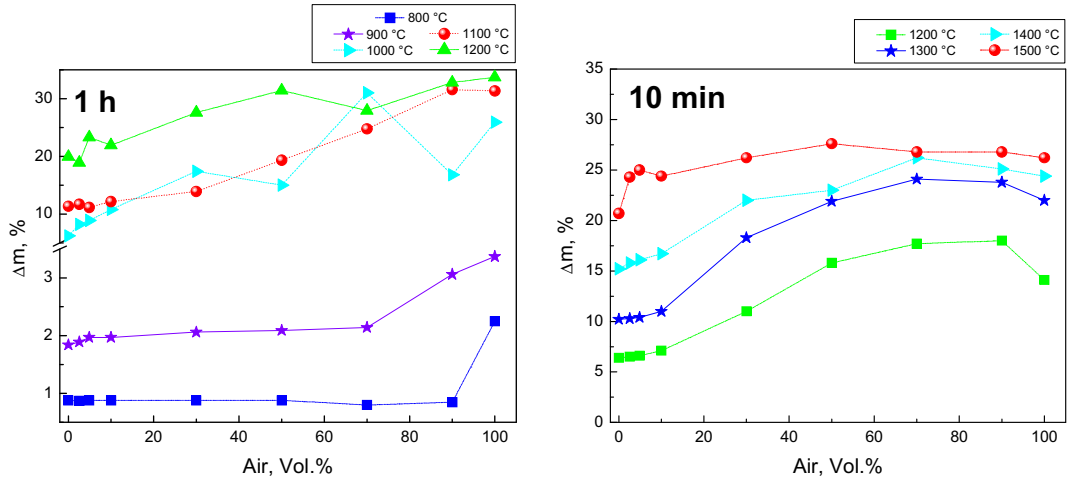

Fig. 7. Mass gain of specimens after isothermal tests for 1 h at 800–1200 °C (left) and 10 min at 1200–1500 °C (right) as a function of the composition of the air–steam mixture.

kinetics. The breakaway effect causes the variations in the curve of the 1000 °C series, which is also higher than those of the series run at the other temperatures. The curves of the 10-min test at the higher temperatures (Fig. 7, right) are continuous with maxima at ~80% air. The dependence of oxidation on the composition of the atmosphere decreases with temperature and is remarkably small in the 1500 °C test series.

These results are confirmed by the post-test examinations. Macro- and micrographs of all 81 specimens are compiled in [10]. Here, only some characteristic images from tests at various temperatures will be shown. As already obvious from the mass gain diagram (Fig. 7), the addition of air to steam had no effect on the oxidation of Zircaloy-4 during the 1-h isothermal tests at 800 °C. A significantly higher mass gain was obtained for pure air only, which is also confirmed by the post-test examinations. The oxide scale of this specimen was much thicker and more porous than that of all other specimens of this series. Small amounts of gold-colored nitride were observed in the oxide scale near the metal–oxide phase boundary. No nitride was found in all other specimens oxidized at 800 °C. A undulating interface between metal (α-Zr(O)) and oxide in all specimens indicated pre-breakaway conditions.

The influence of air in the atmosphere was stronger at 900 °C (Fig. 8). Locally significant nitride formation near the metal–oxide interface was observed for pure air as well as for 90/10 and 70/30 air–steam mixtures. Much smaller amounts of nitrides were seen when the air content was reduced down to 30 vol.%. Less air in the mixture had no effect on the quality of the oxide scale. At 1000 °C, the influence of air on the degradation of Zircaloy during oxidation increased dramatically. Nitride phases were found in all specimens except for those oxidized in pure steam. Almost complete oxidation occurred in pure air and in the 90/10 and 70/30 mixtures, but strongly enhanced degradation was also found for the 50/50 mixture.

The micrographs in Fig. 9 again reveal the initiation of nitride formation at the oxide–metal interface of specimens oxidized in pure air and the mixtures as well as the characteristics of breakaway oxidation with an undulating phase boundary and circumferential cracks in the oxide layer. Dark-field images show rather different oxide morphologies near the metal and near the external surface. The oxide near the external surface is not (no longer) mixed with nitride and exhibits numerous microcracks. The outermost oxide scale of about 30 μm in thickness is of columnar structure and was formed first before the transition to breakaway oxidation and nitrogen attack.

The specimens were completely oxidized after the 1-h tests at 1100 and 1200 °C in air and in mixtures with a high air content. At these and higher temperatures, breakaway oxidation did not occur and the metal–oxide interface of specimens with less than 50% air at 1100 °C and <30% at 1200 °C in the mixture was smooth and no nitrides were observed. Nevertheless, degradation was found to increase gradually with the air content in the mixture, which is also evident from the photos of the specimens after one hour of oxidation at 1200 °C in Fig. 10.

The attack of nitrogen takes place locally at cracks or other imperfections in the oxide scale as can be seen from the images of the short-term tests, e.g., in Fig. 11. After 10 min at 1300 °C in a 30/70 air–steam mixture (here, as an example), local defects

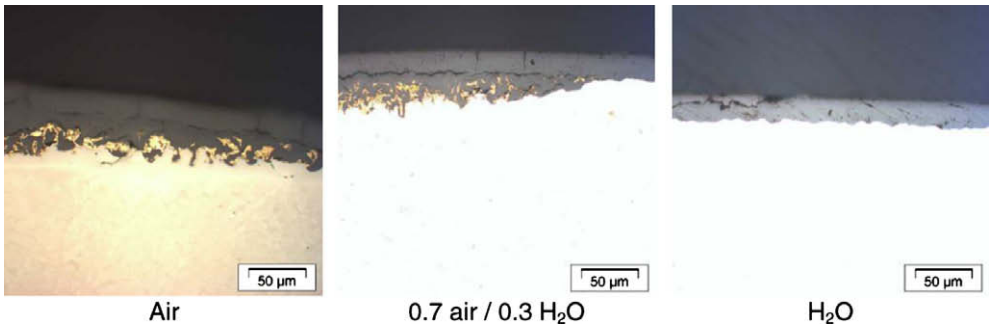

Fig. 8. One hour, 900 °C: optical micrographs of selected specimens.

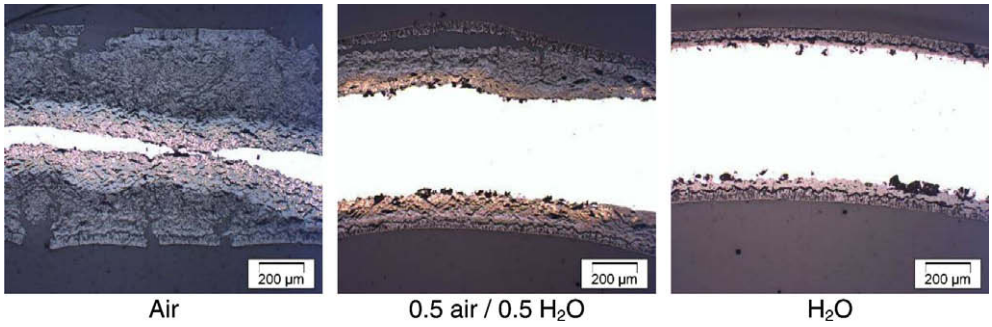

Fig. 9. One hour, 1000 °C: Optical micrographs of selected specimens.

Fig. 10. Post-test appearance of specimens oxidized at 1200 °C in mixed air–steam for 1 h.

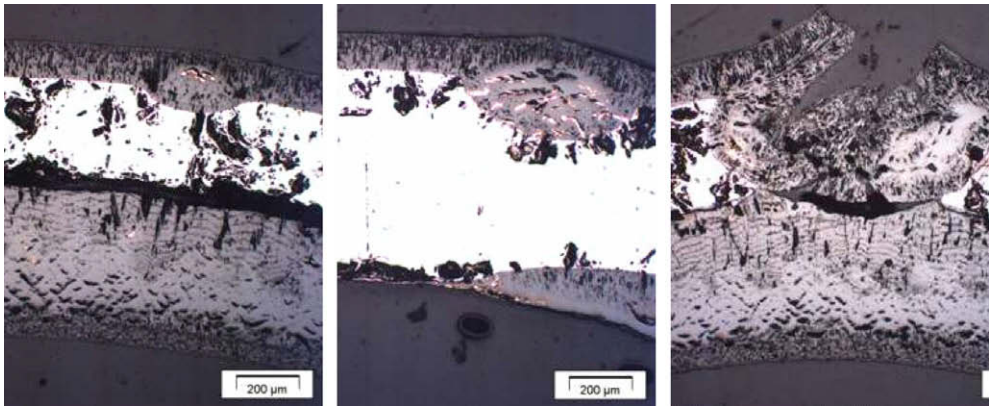

Fig. 11. Images taken at different positions of the specimen after 10 min oxidation at 1300 °C in a 30/70 air–steam mixture.

were caused by a nitrogen attack at different positions of the same specimen in different states of development. Clearly, first access of nitrogen via defects in the oxide occurred at different times. The degraded areas consisted of oxide–nitride mixtures or, in the later stage, (right in Fig. 11) only of porous oxide formed by the re-oxidation of nitride.

3.3. Kinetic investigations in 50/50 air–steam atmosphere

The results presented in the previous section are mainly of phenomenological nature. In the test series with mixed air (nitrogen)–steam atmospheres, only one data point per temperature and gas composition was obtained. For this reason, the test program was extended by experiments in 50/50 air–steam mixtures that are typical of reactor accident scenarios [5], the objective being to determine kinetic correlations [14].

At 800 and 1000 °C, transition from parabolic to faster kinetics was observed after about 10 h and 50 min, respectively. At higher temperatures, by contrast, oxidation could be described by parabolic correlations until almost complete oxidation, as can be seen in Fig. 12. The parabolic rate constants given in Fig. 13 were calculated excluding the post-transition ranges and excluding the data near complete oxidation. The comparatively low value of the mass gain rate constant at 1400 °C correlates with the tendency of a reduced nitrogen attack at temperatures from 1400 °C as described above.

Fig. 14 shows that at 800 °C after about 50 min and at higher temperatures from the very beginning, the admixture of air significantly enhances oxidation, here represented by the oxide scale thickness.

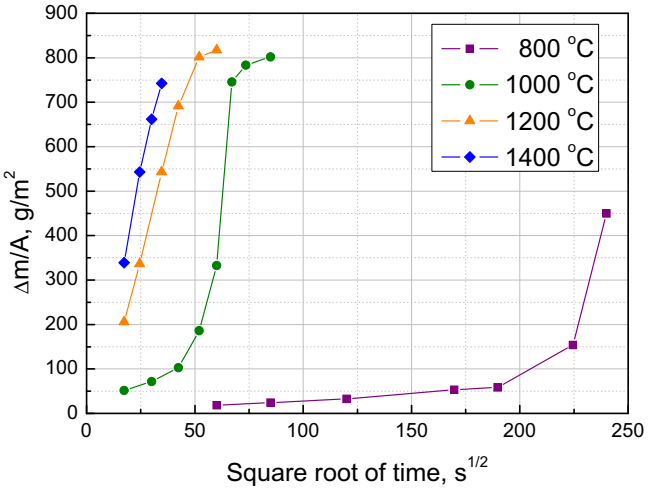

Fig. 12. Weight gain of Zry-4 specimens oxidized in 50/50 air–steam mixtures.

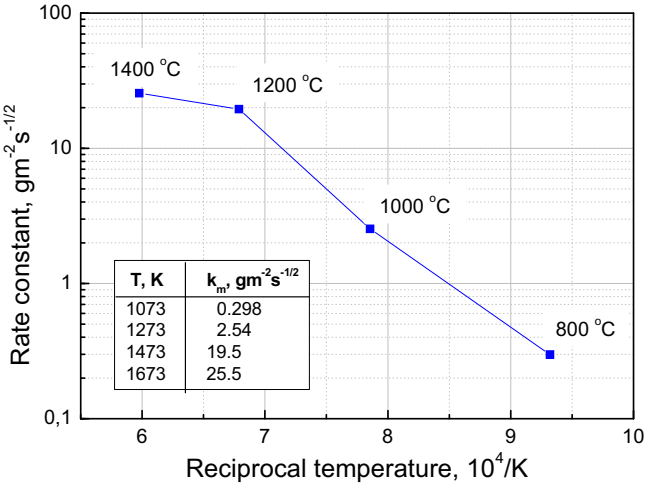

Fig. 13. Parabolic rate constants of Zry-4 oxidation in 50/50 air–steam mixtures.

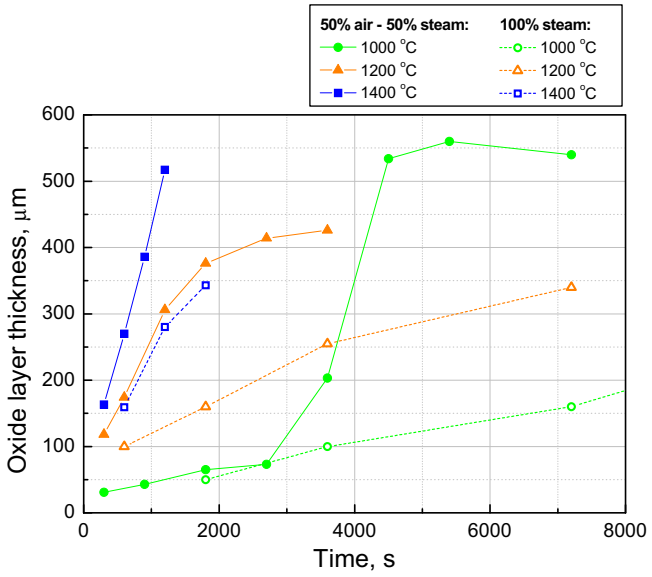

Fig. 14. Oxide layer thicknesses after oxidation of Zry-4 in pure steam and in 50/50 air–steam mixtures at 1000, 1200, and 1400 °C.

3.4. Tests in mixed nitrogen–steam atmospheres

Tests similar to those described in the previous chapters were performed in nitrogen–steam mixtures. Such atmospheres may be present: (1) when all oxygen is consumed in the lower part of a fuel bundle, i.e., under oxygen starvation conditions and (2) in BWRs where containments are filled with nitrogen for inertization, and safety injection systems are pressurized by nitrogen.

This test series was less extensive than the previous one. Isothermal tests were conducted at 1000 °C (1 h), 1200 °C (1 h, 10 min), and 1400 °C (10 min) in pure steam, in steam–nitrogen mixtures with 10, 50, and 95 vol.% nitrogen, and in pure nitrogen.

The offgas composition was measured by MS. The main gas of interest was hydrogen, because it is an indicator of the reaction kinetics. At 1000 °C and high and medium steam contents, the reaction started with a parabolic kinetics developed into a much faster one after 33 and 9 min, respectively. This was due to the breakaway effect that was accelerated by the presence of nitrogen. A more or less linear behavior was observed for the mixture with 95% nitrogen. As expected, no breakaway effect was seen at the higher temperatures. The reaction kinetics was somewhere between parabolic and linear, with the tendency towards a more linear behavior at low steam contents in the mixture. Interestingly, the highest amount of hydrogen was produced in tests with 50/50 mixtures. Even during tests with only 5% steam and 95% nitrogen, more hydrogen was produced than in tests under pure steam, as is evident from Fig. 15.

The mass gain vs. nitrogen concentration in the gas mixture was very similar to hydrogen release (Fig. 15). Again, maximum values were obtained for the 50/50 mixture. Comparison of the two measurements also revealed that a significant fraction of the mass gain (up to 50%) must have been caused by the uptake of nitrogen.

As already seen in Fig. 15, oxidation and so degradation of the specimens was strongest during tests in 50/50 mixtures. After the test for 1 h at 1000 °C, the Zry-4 tube segment was strongly swollen by more than 30%. After the 1200 °C test (1 h), the specimen was so brittle that it broke into pieces during handling. Both specimens were almost completely oxidized. Though less pronounced, this tendency was also seen after the 10-min tests at 1200 and 1400 °C. After annealing in 50/50 mixtures, these specimens possessed the most degraded surfaces.

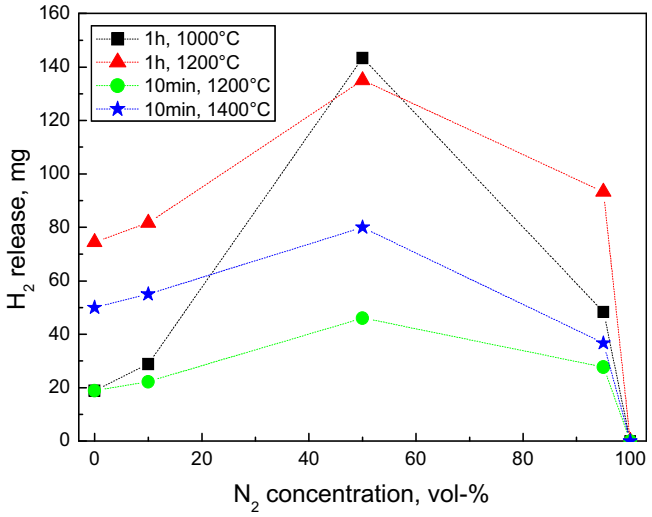

Fig. 15. Integral hydrogen release during the isothermal reaction of Zircaloy-4 in nitrogen–steam mixtures.

The metallographies are quite similar to those of specimens exposed to mixed air–steam atmospheres. The degradation of the oxide scales is even more pronounced after treatment of Zircaloy-4 in nitrogen–steam mixtures compared with air–steam, especially at 1000 °C. Except at the high temperatures (1200, 1400 °C) and low nitrogen content (10%), the oxide scales are very porous and cracked. Nitride precipitates were found in the oxide scale near the metal–oxide phase boundary. Local nitrogen attack was observed in particular in the short-term tests. In addition, coarsening of the oxide microstructure was observed with rising temperature. Metallographies of the series with 50% and 95% nitrogen in the mixture are presented in Fig. 16.

3.5. Influence of pre-oxidation on subsequent oxidation in air and nitrogen

Direct access of air to the metallic cladding during any kind of hypothetical accident in nuclear reactors, storage pools, or transport casks is very unlikely. This is because the cladding tubes will have already been oxidized in water/steam during operation and/or the initial phase of the accident. For this reason, a separate-effects test program was performed to study the influence of pre-oxidation on the reaction in air and nitrogen. Particular interest focused on the extent to which an oxide scale formed in steam can protect the cladding from a nitrogen attack and the associated strong degradation described in the previous sections.

The majority of these experiments were conducted in the thermal balance with pre-oxidation in argon–oxygen mixtures. Only one test series at 1200 °C was performed in the BOX rig with pre-oxidation in steam in order to confirm the similarity of steam and oxygen. Tests were run without and with pre-oxidation, with the degree of pre-oxidation serving as parameter.

To start the program, a series of 80 min isothermal tests at 1100 °C was performed under oxygen, air, and nitrogen, with and without pre-oxidation. For comparison, a test with pre-oxidation and subsequent oxidation in air at 1000 °C was carried out. The results of these tests are described in [8] and can be summarized as follows: Pre-oxidation at high temperature prevents nitrogen attack during subsequent oxidation in air, as long as the oxide scale is dense, but strongly enhances the reaction with nitrogen during subsequent reaction in the nitrogen atmosphere.

Later on, numerous systematic experiments were run at temperatures of 800, 1000, 1200, and 1400 °C in the thermal balance to study the influence of pre-oxidation in oxygen on the subsequent reaction in air and nitrogen. Most of the experiments were performed using open specimens. Owing to the different behavior of the inner and outer surfaces of these specimens especially after short pre-oxidation times, some tests were conducted with specially prepared closed specimens (see Section 2.2).

At 800 and 1000 °C, i.e., in the breakaway regime, pre-oxidation caused a delay of the transition from parabolic to linear or even faster kinetics. The left diagram in Fig. 17 shows that the TG curves in air initially follow the curve obtained in pure oxygen. After a delay of about 5000 s, the reaction rates increase and agree with the curve obtained in pure air. Optical micrographs [10] show strongly degraded oxide scales with an initially formed dense external layer and nitride precipitates near the oxide–metal boundary. Nitrogen attack is obviously due to the breakaway effect.

At higher temperatures (1200, 1400 °C), pre-oxidation prevents the specimen from being attacked by the nitrogen, and the oxidation kinetics continues to be parabolic even after the change from oxygen to air flow, as it is demonstrated by the right diagram in Fig. 17. The pre-oxidation phase in these tests was very short compared with the total duration of the experiments.

In comparison with fresh metal, reaction rates in nitrogen are significantly higher after pre-oxidation in oxygen, but seem to be independent of the degree of pre-oxidation, as can be seen from Fig. 18. By way of an example, the diagram compares the reaction rates, $d(\Delta m)/dt$, of Zircaloy-4 in pure nitrogen as a function of the degree of pre-oxidation at 1200 °C. This behavior was observed at all temperatures investigated. Contrary to the tests in air, gold-colored nitride phases were formed mainly at the external surface of the oxide layer (see Fig. 19).

A test series at 1200 °C was performed in the BOX rig with pre-oxidation in steam and subsequent reaction in air and nitrogen, in order to verify the assumption of pre-oxidation in oxygen and steam being very similar. All tests took 50 min with 0, 1, and 5 min pre-oxidation in steam. For comparison, three specimens were oxidized in steam only for 1, 5, and 50 min. This test series confirmed the results obtained in the thermal balance with pre-oxidation in oxygen. The oxide scale formed during pre-oxidation protected the metal from attack by nitrogen in case of a subsequent reaction in air. Pre-oxidation and the following reaction in nitrogen led to a strongly degraded oxide scale that was almost completely converted into nitride.

3.6. Tests to study the mechanisms of nitrogen attack

The results presented in the previous sub-sections indicate that significant nitrogen attack occurs only in the absence of oxygen in the gas phase (local or global oxygen starvation, see below) and in the presence of oxygen in the solid phase. From the thermochemical point of view, stoichiometric zirconia is supposed to be stable in a nitrogen atmosphere. Nitrogen was therefore assumed to attack hypostoichiometric oxide or zirconium with dissolved oxygen. Oxygen stabilizes the hexagonal α-Zr(O) phase which is able to dissolve up to about 30 at.% oxygen, as is shown in the Zr–O binary phase diagram, Fig. 20.

Five Zircaloy-4 specimens with different oxygen contents were annealed in nitrogen at 1200 °C to check which phase was accessible for nitrogen reaction: Pure Zry-4, β-Zr with about 3 at.% oxygen, α-Zr(O) with about 26 at.% oxygen, hypostoichiometric oxide $ZrO_{1.9}$ and stoichiometric ZrO_2, as indicated by the arrows in Fig. 20. In the thermal balance the specimens were subjected to: (1) slow oxidation at 1200 °C until the desired mass gain was obtained, (2) 3 h of homogenization in argon at 1400 °C, and (3) 1 h of reaction at 1200 °C in nitrogen. Reference specimens were prepared by cooling down the TG furnace after step 2.

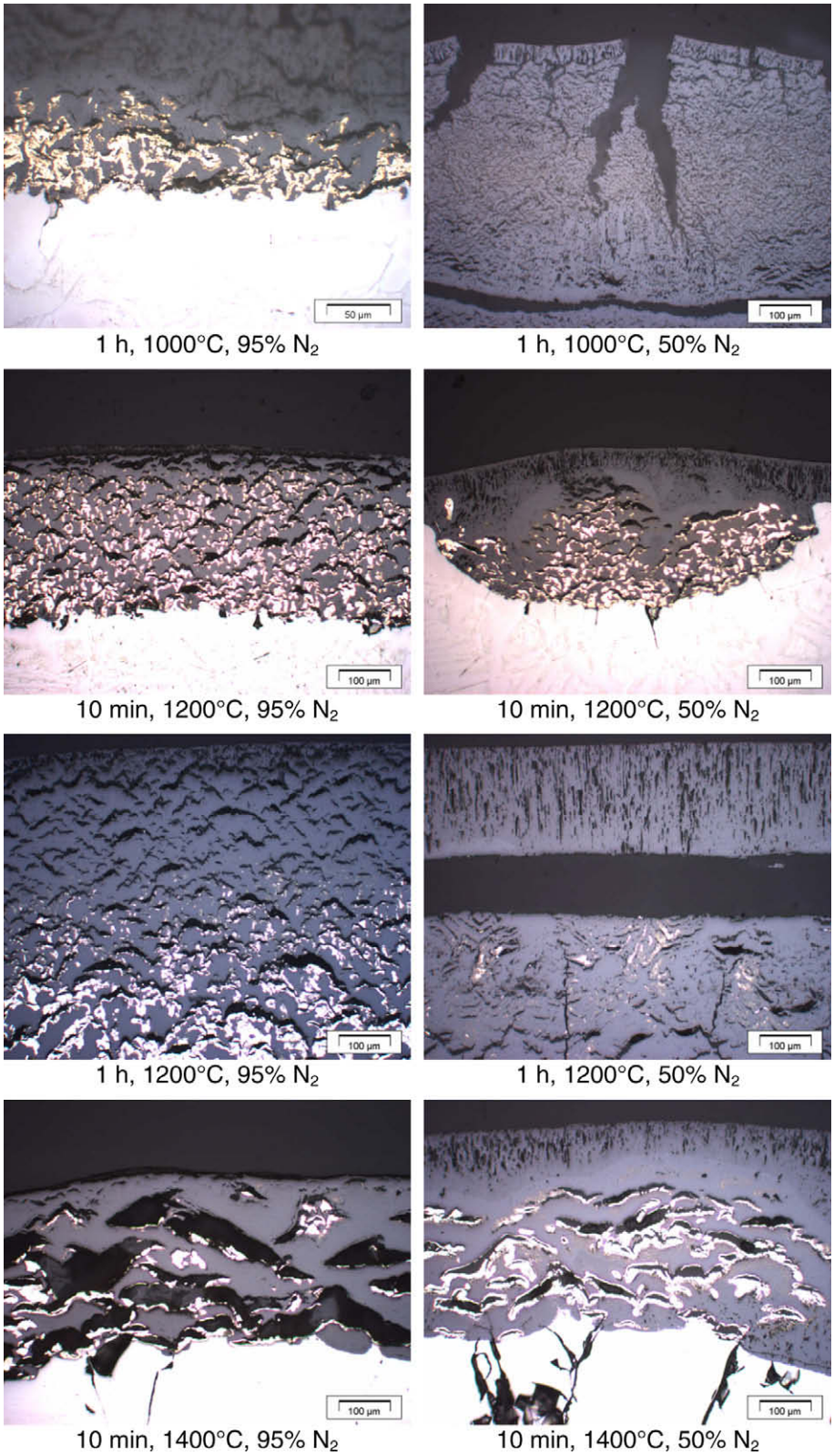

Fig. 16. Optical micrographs of Zircaloy-4 specimens after oxidation in 95/5 and 50/50 nitrogen–steam mixtures.

In Fig. 21 the TG signals of all tests are compared with nitrogen access starting with the initiation of nitrogen injection. The highest mass gain by far was exhibited by the α-Zr(O) specimen. Saturation was reached after about 1000 s. The second fastest reaction was observed for the hypostoichiometric oxide. By nature, the capacity for further nitrogen uptake was limited. A nitride scale covered the surface of the specimen and open cracks. Finally, both specimens were 'oxidized' completely, i.e., no metal was left. The mass gain of α-Zr(O) was 5.7% during oxidation and 12.8% during the nitrogen phase, thus yielding a final composition of $ZrO_{0.325}N_{0.881}$. The

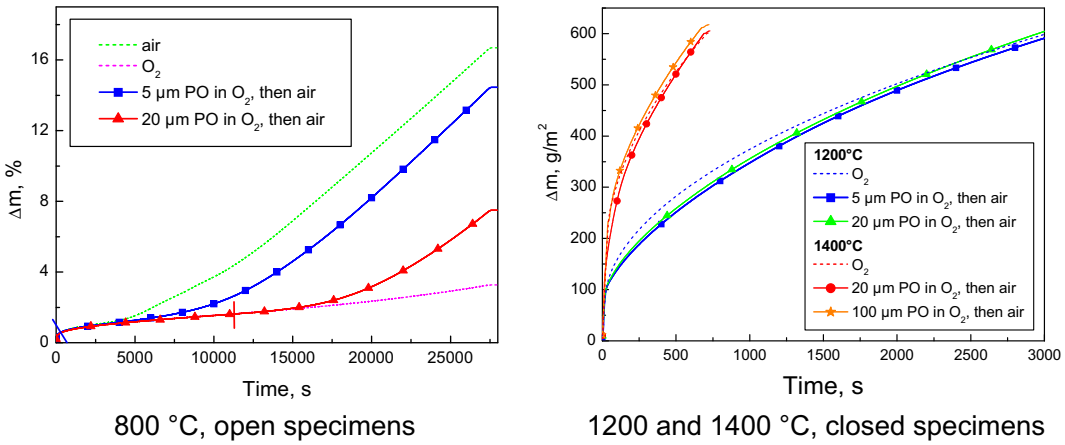

Fig. 17. Influence of pre-oxidation (PO) on subsequent oxidation in air. The vertical lines in the left diagram indicate the transition from pre-oxidation in oxygen to reaction in air.

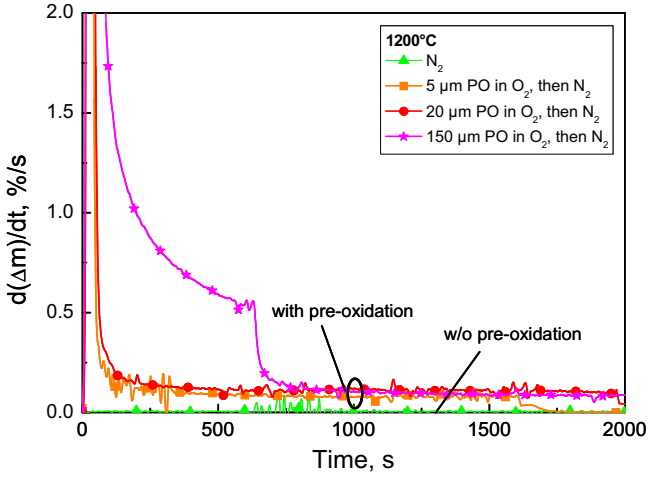

Fig. 18. Influence of pre-oxidation on subsequent oxidation in nitrogen.

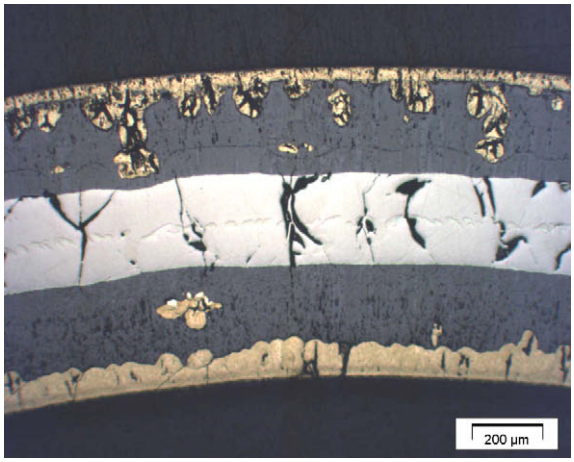

Fig. 19. Micrograph of a Zircaloy-4 specimen after 10 min of pre-oxidation in oxygen and 52 min in nitrogen. External nitride formation is visible.

optical micrographs in Fig. 22 reveal the formation of a ZrO_2–ZrN two-phase mixture, i.e., the final composition of the specimen is rather 0.16 ZrO_2 + 0.88 ZrN. A small amount of mutual dissolution cannot be excluded.

As already discussed above, pure Zry-4 barely reacts with nitrogen. The same was observed for the β-Zr(O) specimen. As expected, the stoichiometric oxide did not change during annealing in nitrogen.

4. Discussion

The experimental results presented in Section 3 clearly show the strong effect of air and especially of nitrogen on the oxidation and degradation of the Zircaloy cladding. Generally, air in the atmosphere can dramatically increase degradation, such that the cladding barrier effect against the release of fission products is lost much earlier than under pure steam conditions.

The reaction kinetics in pure oxygen, nitrogen, and air largely differ from each other. Oxidation of zirconium alloys in oxygen is similar to that in steam. It is characterized by the formation of a protective oxide scale and, thus, controlled by the diffusion of oxygen through the growing oxide layer. This results in parabolic kinetics. At temperatures below 1100 °C, this is true for the initial period only, before a transition to a faster, more complicated, but rather linear kinetics occurs due to the breakaway of the oxide scale. In air this transition occurs much earlier and the kinetics is much faster than in steam and not limited to the breakaway regime. Interestingly, a reversal of the increasing degradation with temperature in air is observed at temperatures of 1400–1500 °C. This can be explained by the increasing plasticity of the oxide with temperature, as a result of which stresses built up by initial nitride formation are only partially relieved by crack formation.

The reaction kinetics of as-received Zry-4 in nitrogen was parabolic at all temperatures investigated, but much slower than in the oxygen-containing gases. Nitride phases were not detected in the metallographic post-test analyses, only a comparably thin α-Zr(N) phase was observed in specimens annealed in pure nitrogen.

A considerable nitrogen attack, i.e., extremely porous oxide layers with nitride precipitations, was also observed in air–steam and nitrogen–steam mixtures of a large composition range. Degradation increased with increasing temperature (at least up to 1300 °C) and an increasing content of air in the mixture. The maximum degradation of the Zircaloy-4 cladding in nitrogen–steam was found for 50/50 mixtures.

Nitride formation in these tests was always observed in the oxide near the metal–oxide boundary. The attack started locally from defects in the oxide scale, where the air can diffuse, e.g., through cracks to the oxide–metal interface. There, the oxygen was consumed first and a pure nitrogen atmosphere remained, which then reacted either with the α-Zr(O) phase or the hypostoichiometric oxide

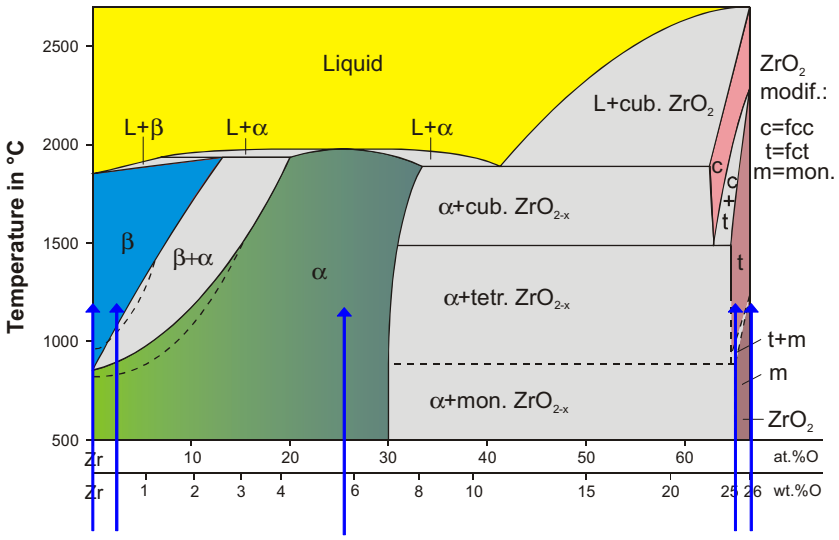

Fig. 20. Zr–O binary phase diagram. The arrows indicate the compositions of the specimens prepared and investigated.

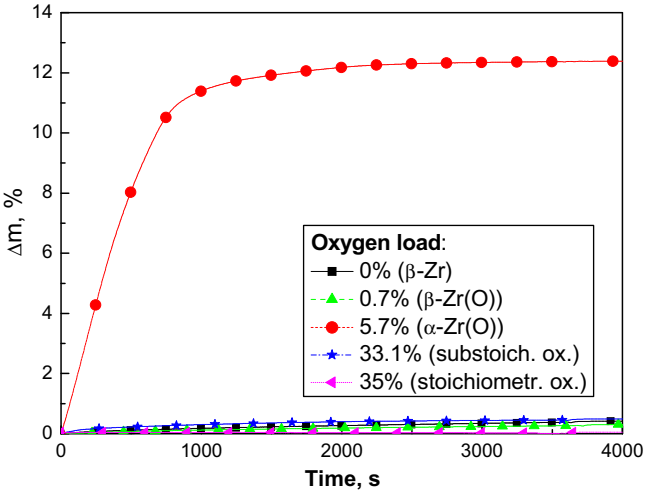

Fig. 21. Mass gain of pre-oxidized and homogenized Zircaloy-4 specimens during annealing in nitrogen at 1200 °C.

existing here. Nitride formed under local oxygen starvation. As the oxide scale grew further, the formed nitride 'moved' outwards and was re-oxidized by fresh air flowing from the external surface to the metal. Owing to the lower density of ZrO_2 (5.6 g/cm^3) in comparison with ZrN (7.1 g/cm^3), this reaction was associated with a significant volume increase (48%) leading to high compressive stresses which are relieved by the formation of cracks. Incidentally, a volume mismatch already occurred during nitride formation and caused the formation of pores.

Fig. 23 illustrates this mechanism. Three regions in the oxide layer can be distinguished. The internal region with nitride precipitates is characterized by macrocracks formed during breakaway oxidation and/or nitride formation, and the external region is interspersed with microcracks that are revealed by dark-field illumination. The outermost oxide layer, about 30 μm thick, is of columnar structure and was formed during the pre-oxidation period before the transition to breakaway and nitrogen attack.

Below 1100 °C, breakaway oxidation and nitride formation mutually accelerate each other. Breakaway-induced failures in the oxide scale allow for an early access of the nitrogen to the metal–oxide interface, leading to the formation of nitride as discussed above. This effect is especially pronounced in the 800 °C tests described in Section 3.1, where the mass gain is larger by far and the oxide scale is much thicker in air than in oxygen-annealed samples. By the way, the mechanisms of breakaway and air attack are quite similar. Both are connected with volume mismatches caused by the tetragonal-monoclinic phase transition during 'pure' breakaway [11] and by the formation and oxidation of nitride during the reaction in air.

Generally, nitrogen attack takes place locally at places where the oxide is defective and air/nitrogen can access the metal. This

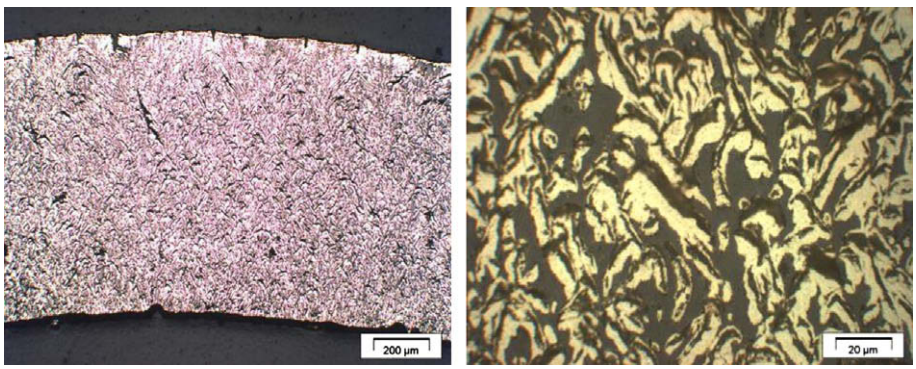

Fig. 22. Wall cross-section and magnified image (10× higher) of the specimen with 5.7% PO after subsequent annealing in nitrogen.

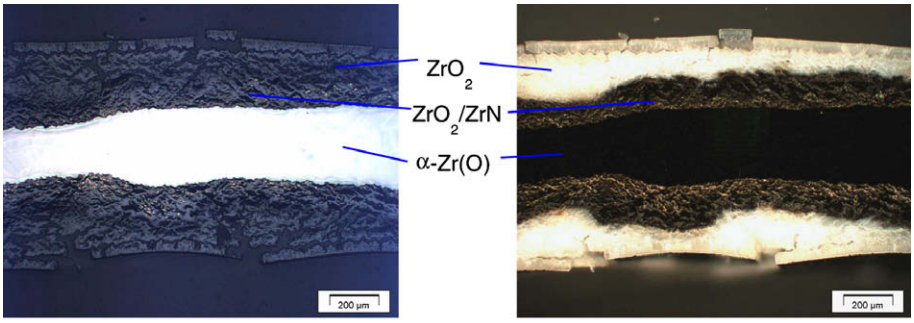

Fig. 23. Optical micrographs of a Zry-4 cladding after pre-oxidation in oxygen and oxidation in air at 1000 °C. The dark-field image reveals the presence of microcracks in the external part of the oxide, where the nitride has already been re-oxidized.

is illustrated e.g. by the micrographs of the 10-min tests at 1200–1400 °C in mixed atmospheres (Figs. 5 and 11). First nitrogen attack causes fast (increasing with temperature and time) proliferation of the area affected, which eventually results in the complete degradation of the scale. Local defects are also reflected by bumps and spots at the surface of these specimens in the macroimages. At temperatures below 1100 °C, degradation of the oxide layers on specimens annealed in an air-containing atmosphere is more layer-like, because the crack-network resulting from breakaway offers a more homogeneous area for nitrogen attack.

An intact oxide scale, even a thin one, formed before air ingress may effectively protect the cladding from nitrogen attack and the associated degradation. During annealing in air, the scale continues to grow as before in oxygen as long as the access of nitrogen to the metal is blocked and as long as oxygen is available. A protective oxide scale is of course only formed beyond the breakaway regime, i.e., above ca. 1050 °C.

Global oxygen starvation, i.e., the absence of oxygen or other oxidizing gases in the atmosphere, changes the situation significantly. In experiments with pre-oxidized Zircaloy specimens in pure nitrogen, large amounts of nitrides were formed externally in the oxide scale independently of the degree of pre-oxidation. Stuckert [12] reports that oxygen diffusion from the oxide to the metal occurs under steam starvation conditions, leading to the formation of hypostoichiometric oxide, α-Zr(O) precipitations in the oxide, and even external α-Zr(O) layers on the oxide. Although the oxide is thermodynamically much more stable than the nitride, nitrogen may react with hypostoichiometric oxide and the α-Zr(O) phase, as was shown in Section 3.6.

The results of these experiments also explain why pure metal reacts insignificantly with nitrogen, but strong nitride formation is observed during the reaction of Zircaloy in air. At the metal–oxide interface, α-Zr(O) and ZrO_{2-x} are available, which both rapidly react with the attacking nitrogen. It was also shown in these experiments that β-Zr with no or a low oxygen content only insignificantly reacts with nitrogen. The reason is not yet clear. It is assumed that nitrogen occupies lattice defects in the hypostoichiometric oxide or the Zr–O solution, resulting in the formation of nitride seed crystals.

Table 1 summarizes the influence of pre-oxidation in oxygen/steam on the subsequent reaction in air and nitrogen. This is only valid at temperatures above 1050 °C. Especially for reactions in air, deviations from the linear kinetics to slower and faster ones were found.

Table 1
Reaction kinetics of Zircaloy-4 in oxygen, air, and nitrogen with and without pre-oxidation in steam or oxygen.

Pre-oxidation	Reaction in		
	Oxygen/steam	Air	Nitrogen
No	Parabolic	Linear (fast)	Parabolic (slow)
Yes		Parabolic	Linear

5. Summary and conclusions

The paper presented the results of extensive experiments relating to the oxidation of Zircaloy-4 in air-containing atmospheres at high temperatures. The experimental program was aimed at determining the mechanistic phenomenology of the reaction between Zircaloy and air and at investigating air attack under prototypical conditions of air ingress during a hypothetic severe nuclear reactor accident, i.e., at temperatures between 800 and 1500 °C. Mixed air (nitrogen)–steam atmospheres and pre-oxidation were also taken into consideration.

Oxidation in air as well as in air- and nitrogen-containing atmospheres leads to strong degradation of the cladding material. The main mechanism is the formation of zirconium nitride and its re-oxidation. The different densities of Zr, ZrO_2, and ZrN cause volume mismatches, compressive stress build-up, and relief by crack formation leading to porous, non-protective oxide scales. From the safety point of view, the barrier effect of the fuel cladding is lost much earlier than during accident transients under an atmosphere that consists of steam exclusively.

Significant formation of ZrN took place under local or global oxygen starvation conditions, i.e. in the absence of oxygen/steam in the gas phase, and the presence of oxygen in the solid phase. α-Zr(O) and, to a limited extent, the hypostoichiometric oxide ZrO_{2-x} then react with nitrogen to form zirconium nitride.

Pre-oxidation in steam prevents air from attacking as long as the oxide scale is intact, i.e. at temperatures above 1050 °C (beyond the breakaway regime) and as long as oxidizing gases are available (absence of steam starvation conditions).

Under steam/oxygen starvation conditions, the oxide scale is reduced (both chemically and with respect to its thickness) and significant external nitride formation takes place. From the point of view of safety, this nitride may very rapidly re-oxidize during reflooding with water, which may result in temperature escalations in a later phase of the accident.

More generally, the high exothermal energy of the oxidation of zirconium alloys in air, on the one hand, and the small cooling effect of air compared to steam, on the other, cause early temperature escalations from relatively low temperatures, as was seen

during the preparation and conduct of the QUENCH-10 bundle test relating to air ingress [9].

As regards the modeling of air ingress in severe accident computer codes, it is concluded that parabolic correlations for oxidation in air may be applied only for high temperatures (>1400 °C) and for a pre-oxidized cladding ($\geqslant$1100 °C). For all other conditions, faster, i.e., rather linear reaction kinetics should be applied.

Acknowledgements

The work reported here is funded under the HGF NUKLEAR Program of Forschungszentrum Karlsruhe. The experiments were partly performed by T. Ziegler within the framework of her diploma thesis work and by the guest scientist N. Vér (AEKI Budapest) under EC SARNET mobility program. The author would like to thank P. Severloh and U. Stegmaier (FZK) for performing metallographic examinations, G. Schanz and M. Große (FZK) for very fruitful discussions, and M. Schröder for the thorough English review of the report.

References

[1] D.A. Powers, L.N. Kmetyk, R.C. Schmidt, A Review of Technical Issues of Air Ingression during Severe Reactor Accidents, Report NUREG/CR-6218, SAND94-0731, Sandia National Lab., 1994.
[2] I. Shepherd et al., Oxidation Phenomena in Severe Accidents (OPSA), Final Report, INV-OPSA(99)-P008, 2000.
[3] I. Shepherd et al., Nucl. Eng. Des. 209 (2001) 107.
[4] K. Natesan, W.K. Soppet, S. Basu, Low Temperature Air Oxidation Experiments at ANL, CSARP Meeting, Crystal City, VA, 3–4 May 2004.
[5] P. Giordano, C. Séropian, The Air Ingress Issue for PWRs, Fifth Technical Seminar on the Phebus FP Programme, Aix-en-Provence, June 2003.
[6] C. Duriez, T. Dupon, B. Schmet, F. Enoch, J. Nucl. Mater. 380 (2008) 30.
[7] M. Steinbrück, A. Miassoedov, G. Schanz, Nucl. Eng. Des. 236 (2006) 1709.
[8] C. Duriez, M. Steinbrück, D. Ohai, T. Meleg, J. Birchley, T. Haste, Nucl. Eng. Des. 239 (2009) 244.
[9] G. Schanz, M. Heck, Z. Hozer, L. Matus, I. Nagy, L. Sepold, U. Stegmaier, M. Steinbrück, H. Steiner, J. Stuckert, P. Windberg, Results of the QUENCH-10 Experiment on Air Ingress, Forschungszentrum Karlsruhe, Report FZKA 7087, 2006.
[10] M. Steinbrück, U. Stegmaier, T. Ziegler, Prototypical Experiments on Air Oxidation of Zircaloy-4 at High Temperatures, Forschungszentrum Karlsruhe, Report FZKA 7257, 2007.
[11] G. Schanz, S. Leistikow, in: Eighth International Congress on Metallic Corrosion, Mainz, Germany, ICC/EFC Proceedings, vol. 2, DECHEMA, 1981, p.1712.
[12] J. Stuckert, M.V. Veshchunov, Behaviour of Oxide Layer of Zirconium-Based Fuel Rod Cladding under Steam Starvation Conditions, Forschungszentrum Karlsruhe, FZKA 7373, 2008.
[13] T.B. Massalski, H. Okamoto, P.R. Subramanian, L. Kacprzak, Binary Alloy Phase Diagrams, 2nd Ed., ASM International, Materials Park, OH, 1990.
[14] N. Vér, Determination of kinetic parameters of the oxidation of zirconium alloys in steam/air mixtures, Report AEKI-FRL-2007-401-01/01, Budapest, 2007.